

Differentiation of recurrent astrocytoma from radiation necrosis: a pilot study with $^{13}\text{N-NH}_3$ PET

Zhang Xiangsong · Chen Weian

Received: 20 September 2006 / Accepted: 24 October 2006 / Published online: 22 November 2006
© Springer Science+Business Media B.V. 2006

Abstract Differentiation of posttherapy radiation necrosis from recurrent brain tumor remains a challenging diagnostic problem. The combination of the imaging modalities on the basis of different physiologic mechanisms could improve diagnostic accuracy. The present study assessed the role of $^{13}\text{N-NH}_3$ PET in differentiating recurrent cerebral astrocytoma from radiation necrosis.

Methods Seven patients, who were previously treated with conventional external-beam radiation therapy after surgical resection for cerebral astrocytomas, and showed the enhancing brain lesions on T1-weighted gadolinium-enhanced MR studies performed in 6 months or above after the radiotherapies, were examined prospectively with $^{13}\text{N-NH}_3$ and FDG PET. Five lesions with tumor recurrence and two with radiation necrosis were histologically verified by either surgical resection or stereotactic biopsy. One lesion of radiation necrosis was confirmed clinicoradiologically.

Results In all eight lesions the $^{13}\text{N-NH}_3$ PET scans were concordant with the final diagnosis (100%, 8/8). The lesions with recurrent tumor showed moderately to markedly increased $^{13}\text{N-NH}_3$ uptake (grade = 4–5). The lesions with radiation necrosis showed absent or less $^{13}\text{N-NH}_3$ uptake than surrounding area (grade = 1–2). The FDG PET scans were concordant with the final diagnosis in six of eight lesions (75%, 6/8), and there were one false-negative result and one false-positive

result. The diagnostic result of $^{13}\text{N-NH}_3$ PET was discordant with FDG PET in two lesions. One lesion with gliosis and radiation necrosis showed slightly increased FDG uptake (grade = 4), but less $^{13}\text{N-NH}_3$ uptake (grade = 2). The other lesion with anaplastic astrocytoma showed moderately increased $^{13}\text{N-NH}_3$ uptake (grade = 4), but slightly less FDG uptake than surrounding area (grade = 2).

Conclusions The recurrent astrocytomas showed increased $^{13}\text{N-NH}_3$ uptake, and the radiation necrosis showed absent or less $^{13}\text{N-NH}_3$ uptake, and $^{13}\text{N-NH}_3$ seem superior to $^{18}\text{F-FDG}$ for this purpose, suggesting that $^{13}\text{N-NH}_3$ is a promising tracer for separating radiation necrosis from astrocytoma recurrence. However, the patient population in this study was small. Thus, the further studies are needed to settle this issue.

Keywords PET · $^{13}\text{N-NH}_3$ · Astrocytoma · Tumor recurrence · Radiation necrosis

Introduction

Differentiation of posttherapy radiation necrosis from recurrent tumor remains a challenging diagnostic problem, however, and has important implications for the patient's management. Modalities used to assess abnormal lesions in the follow-up of treated brain tumors include CT, MRI, SPECT, and PET. Conventional MRI and CT cannot reliably separate radiation necrosis from recurrent tumor for the reason that both recurrent tumors and therapy-induced lesions have a similar radiologic appearance owing to alterations of the blood–brain barrier (1).

Z. Xiangsong (✉) · C. Weian
Department of Nuclear Medicine, The First Affiliated
Hospital, Sun Yat-sen University, 58 Zhongshan Road II,
Guangzhou 510080, China
e-mail: sd_zh@163.net

Over the last 20 years, PET has become indispensable for evaluating brain tumors, especially for differentiating of recurrent tumors from radiation necrosis. ^{18}F -FDG was the first PET tracer for this purpose, but attempts with ^{18}F -FDG were only partially successful. Sensitivity is an issue, especially but not exclusively with low-grade gliomas, and false-positive results may occur (2, 3). Therefore, more specific radiotracers should be developed. The ideal tracer for this purpose would reproducibly demonstrate a different accumulation pattern in radiation necrosis from that in tumor, such as no accumulation in radiation necrosis and high accumulation in tumor.

We have reported that there is the substantial uptake of ^{13}N - NH_3 in cerebral astrocytomas, including low-grade astrocytomas, and has the potential to enable differentiation between low-grade astrocytomas and non-neoplastic lesions (4, 5). Thus, ^{13}N - NH_3 PET may be useful in differentiating recurrent cerebral astrocytoma from radiation necrosis. This study was conducted to assess for the first time the role of ^{13}N - NH_3 PET in differentiating recurrent cerebral astrocytoma from radiation necrosis.

Materials and methods

Patients

Seven patients (five men and two women; mean age \pm SD, 37 ± 9 years) were included in the study. All patients were previously treated with conventional external-beam radiation therapy after surgical resection for cerebral astrocytomas, the initial diagnoses in all patients were proved by examination of histologic specimens, and showed the enhancing brain lesions on T1-weighted gadolinium-enhanced MR studies performed in six months or above after the radiotherapies.

^{13}N - NH_3 PET, FDG PET and conventional MR studies (T1WI, T2WI, contrast enhanced T1WI) were obtained in all seven patients. ^{13}N - NH_3 PET and FDG PET were performed not more than 2 weeks after MRI studies.

The study was approved by the hospital ethics committee and each individual participating in the study gave his or her informed consent.

PET and MR imaging

PET scanning was performed using an ECAT HR⁺ scanner (Siemens/CTI). Patients were fasted for at least 6 h before FDG PET scanning. PET images were

acquired with the patients in the supine position. A dose of 370–555 MBq of ^{18}F -FDG or 555–740 MBq of ^{13}N -ammonia was injected intravenously. Emission images were obtained for 15 min, beginning 40 min after ^{18}F -FDG injection or 5 min after ^{13}N -ammonia injection, and a 19-min dynamic scan ($10 \text{ s} \times 12$, $30 \text{ s} \times 4$, and $900 \text{ s} \times 1$) triggered simultaneously with a bolus injection of ^{13}N -ammonia was performed on five of them. Using a germanium-68 source, transmission images were obtained to correct for photon attenuation for 5 min.

All MR imaging examinations were performed with the clinical 1.5-T imaging units (GE/Signal or Siemens/Magnetom vision). Non-enhanced axial T1-weighted and T2-weighted images were performed. T1-weighted gadolinium-enhanced MR images were obtained after administration of 0.1 mmol/kg gadopentetate dimeglumine.

Data analysis

Two experienced nuclear medicine specialists interpreted the ^{13}N - NH_3 and FDG PET examinations, and the contemporaneous MR examination was available in all patients. The PET analysts were blinded to the histological results.

Qualitative visual analysis of the PET images was performed. Any region in one or more of the PET transaxial slices (within the confines of the abnormality defined on the MR examination) that demonstrated increased FDG or ^{13}N - NH_3 uptake relative to the immediately adjacent tissue was graded abnormal and considered indicative of viable tumor. Regions with markedly reduced or absent FDG uptake in those PET transaxial slices in the confines of the tumor region were interpreted as consistent with radiation necrosis. The same regions used in the qualitative analysis were also graded according to a 5-point grading system as proposed by Kim et al. (6), with 1 = totally absent uptake, 2 = slightly less uptake than surrounding area, 3 = same uptake as surrounding area, 4 = slightly to moderately increased uptake compared with surrounding area, and 5 = markedly increased uptake.

The regions of interest (ROIs) were outlined at the site of maximum ^{13}N -ammonia tumor uptake and the contralateral white matter of the centrum semiovale in the trans-axial planes. Counts per pixel in the tumors and white matters were calculated from the ROIs. The tumor-to-white matter (T/W) count ratios were determined on the delayed PET frame, and the average count ratios of tumor-to-white matter on the first twelve PET frames were calculated as the perfusion index (PI) of the tumors.

The lesion size was determined in the contrast-enhanced T1WI. All lesions were sized in two-dimensions in the transaxial plane in which the lesion was the largest. The mean of the two diameters was used as the lesion size.

Results

Eight newly developed enhancing lesions were found in seven patients, the size of lesions ranged from 0.9 to 6.3 cm (mean, 3.1 cm). The final diagnosis was confirmed either histologically or clinicoradiologically. Five lesions with tumor recurrence and two lesions with radiation necrosis were histologically verified by either surgical resection or stereotactic biopsy. One lesion of radiation necrosis was confirmed clinicoradiologically based on that the enhanced lesion was present but unchanged on serial follow-up MR examinations for 29 months, accompanied by asymptomatic during the follow-up period. At recurrence, three cases that had initially been treated as low-grade astrocytomas had changed to anaplastic astrocytoma ($n = 1$) or glioblastoma ($n = 2$). Table 1 summarizes the findings in the seven patients.

In all eight lesions the $^{13}\text{N-NH}_3$ PET scans were concordant with the final diagnosis (100%, 8/8). Five lesions with recurrent tumor showed moderately to markedly increased $^{13}\text{N-NH}_3$ uptake (grade = 4–5). All three lesions with radiation necrosis showed absent or less $^{13}\text{N-NH}_3$ uptake than surrounding area (grade = 1–2) (Figs. 1, 2). The FDG PET scans were concordant with the final diagnosis in six of eight lesions (75%, 6/8), and there were one false-negative scan and one false-positive scan. Four of five lesions with recurrent tumors had slightly to markedly

increased FDG uptake relative to surrounding area (grade = 4–5), one lesion showed slightly less uptake than surrounding area (grade = 2). Two of three lesions with radiation necrosis showed absent FDG uptake (grade = 1), and one lesion showed slightly increased FDG uptake (grade = 4). The T/W ratios of $^{13}\text{N-NH}_3$ for radiation necrosis and recurrent tumors were 0.90 ± 0.05 and 3.56 ± 0.70 , and the T/W ratios of FDG were 0.97 ± 0.45 and 2.41 ± 0.97 , respectively.

The diagnostic result of $^{13}\text{N-NH}_3$ PET was discordant with FDG PET in two lesions. A ring-like contrast-enhanced lesion was found 7 months after surgical resection and conventional external-beam radiation therapy (60 Gy) in the patient with astrocytoma grade II (case 1). The lesion showed slightly increased FDG uptake (grade = 4), but $^{13}\text{N-NH}_3$ uptake in the lesion was less than surrounding area (grade = 2). The histologic samples obtained during surgery showed gliosis and necrosis, consistent with radiation necrosis, only several atypical tumor cells were found near blood vessel in the completely resected specimens after the surgery (Fig. 3). In patient 6, one small contrast-enhanced lesion (size = 0.9 cm) showed moderately increased $^{13}\text{N-NH}_3$ uptake (grade = 4), but slightly less FDG uptake than surrounding area (grade = 2), and it was histologically proved to be anaplastic astrocytoma (Fig. 4).

Discussion

The modalities that have been evaluated to have a role in the differential diagnosis of recurrent brain tumor versus radiation necrosis are magnetic resonance spectroscopy (MRS); blood-volume imaging with echoplanar magnetic resonance; PET, using $^{18}\text{F-FDG}$,

Table 1 Results of $^{13}\text{N-NH}_3$ and FDG scans compared with tumor grade, lesion size, final diagnosis

Case no.	Age (years)	Sex	Tumor grade	Size (cm)	$^{13}\text{N-NH}_3$				FDG			Final diagnosis
					Diagnosis	Grade	T/W	PI	Diagnosis	Grade	T/W	
1	38	M	N	3.9	N	2	0.95	–	T	4	1.48	N ^a
2	22	F	N	2.3	N	1	0.9	0.98	N	1	0.78	N ^b
3	38	M	N	4.3	N	1	0.85	0.94	N	1	0.65	N ^c
4	39	M	IV	2.1	T	5	3.75	–	T	5	3.41	T ^a
5	36	M	IV	6.3	T	5	4.16	3.82	T	4	2.33	T ^b
6	54	F	III	2.8	T	5	3.69	3.26	T	4	2.12	T ^a
			III	0.9	T	4	2.35	2.08	N	2	0.98	T ^a
7	33	M	IV	2.5	T	5	3.84	4.05	T	5	3.22	T ^a

T = tumor, N = radiation necrosis
^a Diagnosis made by surgical resection
^b Diagnosis made by a biopsy
^c Diagnosis made by clinicoradiologically follow-up

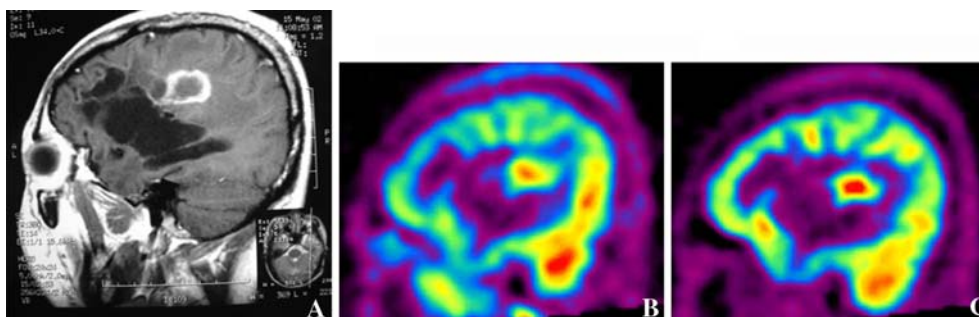


Fig. 1 Thirty nine-year-old man (case 4) who had the resection and radiation therapy of a grade II astrocytoma 3 years ago. (A) T1-weighted gadolinium-enhanced MR image shows a ring-like

enhanced lesion. Both FDG (B) and $^{13}\text{N-NH}_3$ (C) PET showed markedly increased uptake (grade = 5) in the lesion. The lesion was histologically proved to be glioblastoma

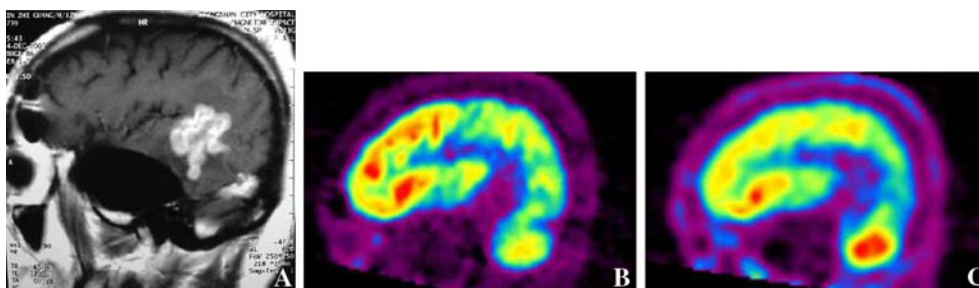


Fig. 2 Thirty eight-year-old man (case 3) who had the resection and radiation therapy of a grade II astrocytoma 2 years ago. (A) T1-weighted gadolinium-enhanced MR image shows an en-

hanced lesion. The lesion showed absent both FDG (B) and $^{13}\text{N-NH}_3$ (C) uptake (grade = 1) in the lesion. The final diagnosis was radiation necrosis made by clinico-radiologically follow-up

^{11}C or ^{18}F -tyrosine, ^{11}C -methionine, and ^{11}C -thymidine; and ^{201}Tl or ^{123}I - α -methyl-L-tyrosine SPECT. The combination of these imaging modalities on the basis of different physiologic mechanisms could improve diagnostic accuracy [1].

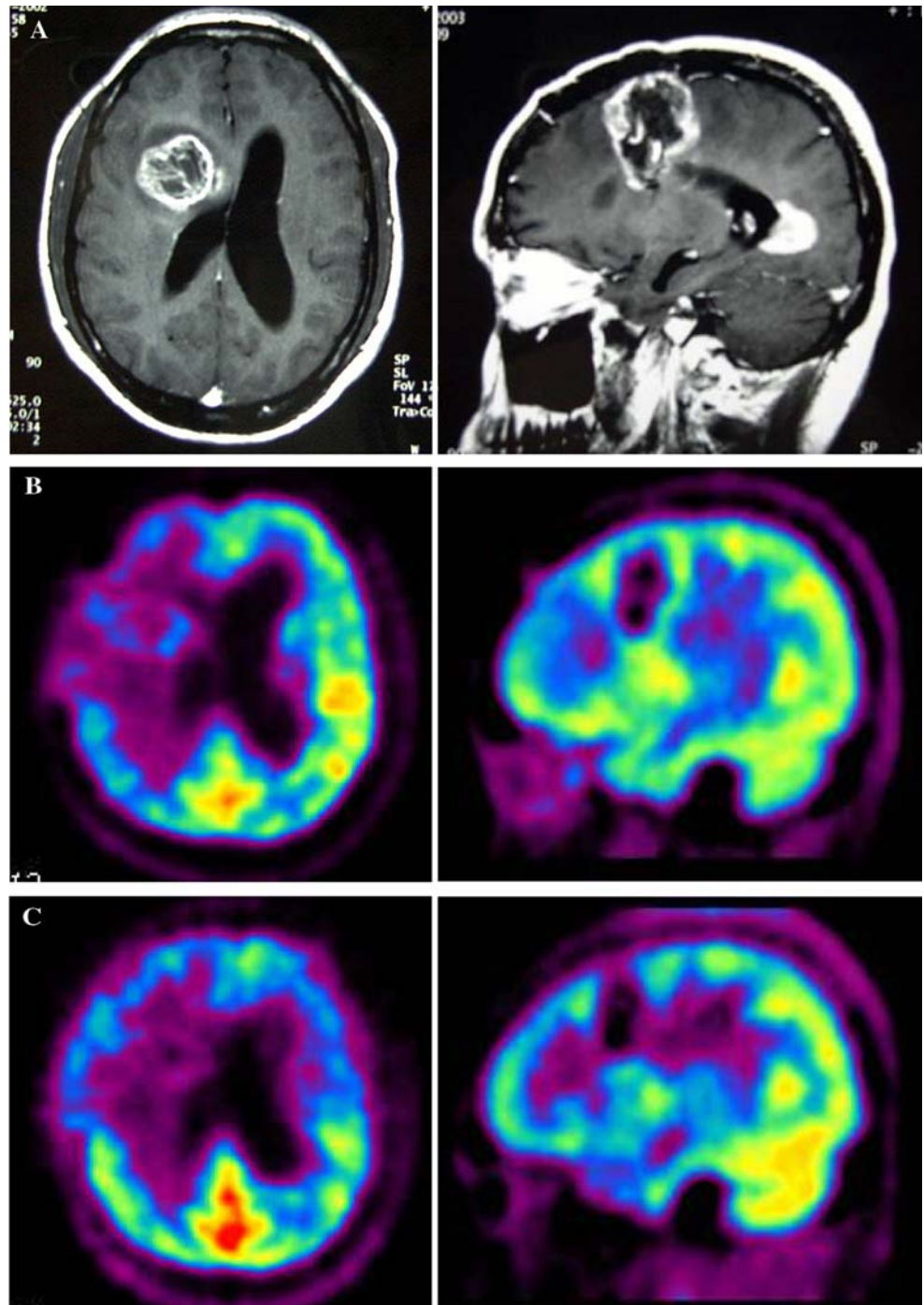
The current prospective study examined for the first time the use of $^{13}\text{N-NH}_3$ PET for differentiation between astrocytoma recurrence and radiation necrosis. In all 8 lesions the $^{13}\text{N-NH}_3$ PET scans were concordant with the final diagnosis (100%, 8/8). The lesions with recurrent tumor showed moderately to markedly increased $^{13}\text{N-NH}_3$ uptake (grade = 4–5). The lesions with radiation necrosis showed absent or less $^{13}\text{N-NH}_3$ uptake than surrounding area (grade = 1–2). The FDG PET scans were concordant with the final diagnosis in six of eight lesions (75%, 6/8), and there were one false-negative result and one false-positive result. The diagnostic result of $^{13}\text{N-NH}_3$ PET was discordant with FDG PET in two lesions. The results suggests $^{13}\text{N-NH}_3$ PET demonstrate a different accumulation pattern in radiation necrosis from that in astrocytoma recurrence, and $^{13}\text{N-NH}_3$ may be an idea tracer for differentiation between astrocytoma recurrence and radiation necrosis.

^{13}N -ammonia has been proved to be a good indicator of brain tissue. Phelps et al. [7] using PET with

normal volunteers, showed that the relative ^{13}N concentrations in structures of the brain were in good agreement with the relative capillary densities and/or cerebral blood flow (CBF). The net ^{13}N -ammonia extraction by brain tissues increases non-linearly with CBF, and depends primarily upon CBF, capillary permeability-surface product (PS) and integrity of the glutamate-glutamine synthetase reaction. The glutamine synthetase reaction is the major route for metabolic trapping of ^{13}N -ammonia in brain tissues [8]. The uptake of ^{13}N -ammonia in brain tumors is probably governed by two main factors: the capillary blood flow in the tumor and the metabolic properties of the tumor [9].

The pathology of late-delayed radiation injury shows fibrinoid necrosis of the medium and small arteries with vascular proliferation [1]. The tumor growth consists of an irregular meshwork of vessels. These vessels markedly differ from those of radiation necrosis, which primarily consist of ischemic changes caused by the endothelial damage. The perfusion-sensitive imaging modalities have been proved to be useful for differentiating highly vascularized recurrent tumor from avascular necrosis. Sugahara et al. [10] concluded an enhancing lesion with a normalized cerebral blood volume (rCBV)

Fig. 3 Thirty eight-year-old man (case 1) who had resection and radiation therapy of a grade II astrocytoma 7 months ago. (A) T1-weighted gadolinium-enhanced MR image shows a ring-like enhanced lesion in the right frontal lobe. (B) FDG PET shows slightly increased FDG uptake (grade = 4) that corresponds to contrast-enhanced areas on MR image. This activity was interpreted as tumor recurrence. (C) $^{13}\text{N-NH}_3$ uptake in the lesion was less than surrounding area (grade = 2), and interpreted as radiation necrosis. A second craniotomy was performed 2 weeks later, and the right frontal lesion was removed. The samples obtained during the surgery showed gliosis and necrosis, and only several atypical tumor cells were found near blood vessel in some completely resected specimens after the surgery

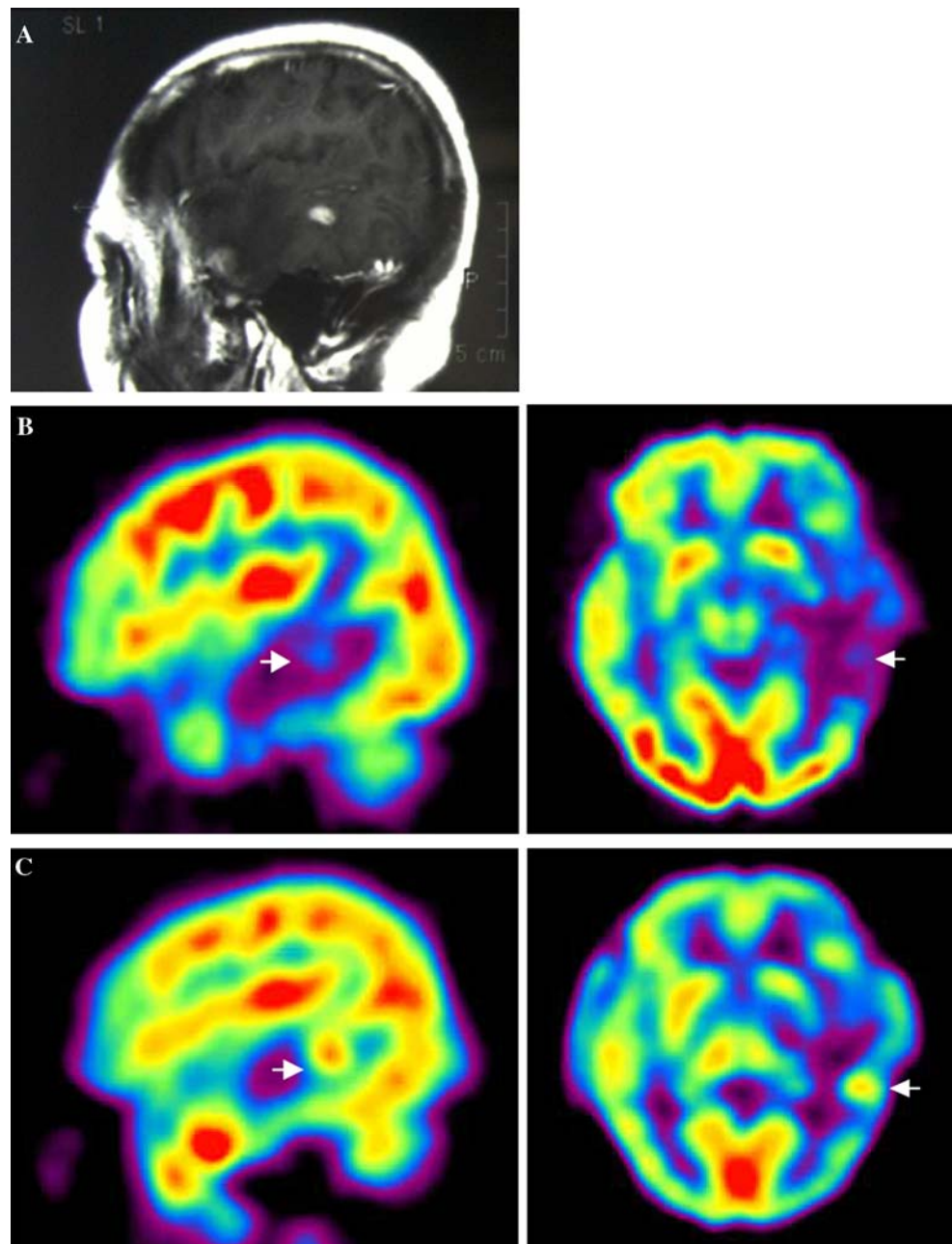


ratio higher than 2.6 or lower than 0.6 may suggest tumor recurrence or non-neoplastic contrast-enhancing tissue using perfusion-sensitive contrast-enhanced MR imaging in the posttherapeutic intraaxial brain tumors. Tsui et al. [11] found that relative regional cerebral blood volume (rrCBV) mapping revealed marked hypoperfusion in radionecrosis of the temporal lobe using dynamic susceptibility contrast MRI in all eight patients with nasopharyngeal carcinoma treated with radiotherapy.

The perfusion agent $^{99\text{m}}\text{Tc}$ -hexamethyl-propyleneamine oxime (HMPAO) was useful in differentiating sites of likely tumor growth from non-specific radiation changes in patients treated for malignant glioma [12, 13].

The glutamine synthetase (GS, L-glutamate ammonia lyase, E.C.6.3.1.2) is oxidatively inactivated by metal-catalyzed oxidation reactions involving the reduction Fe(III) and the production of H_2O_2 [14]. Pilkington et al. [15] found all astrocytomas showed

Fig. 4 Fifty four-year-old woman (case 6) who had resection and radiation therapy of a grade II astrocytoma 12 months ago. **(A)** T1-weighted gadolinium-enhanced MR image shows two contrast-enhanced lesions in the left temporal lobe. **(B)** The big lesion shows moderately increased ^{18}F -FDG uptake was interpreted as tumor recurrence, and the small one shows less FDG uptake, interpreted as radiation necrosis. **(C)** Two lesions showed moderately and markedly increased ^{13}N - NH_3 uptake, interpreted as tumor. Two lesions were histologically proved to be anaplastic astrocytoma



positive staining with GS using the indirect immunoperoxidase and peroxidase-anti-peroxidase methods, the degree of which was related to the extent of differentiation and the amount of cytoplasm of the constituent cells. McCormick et al. and Akimoto also observed the similar results [16, 17]. These results suggest that the GS activity of recurrent astrocytoma is different with the radiation injury, and the inactivated GS caused by radiation and inflammation may decrease ^{13}N - NH_3 uptake in the radiation necrosis.

The perfusion pattern in acute cerebral radiation injury in the rat demonstrated reduced perfusion in the

necrotic center; in the inflammatory layer adjacent to the necrotic center, where ^{18}F -FCH, ^{18}F -FET, and ^{18}F -FDG demonstrated increased uptake, perfusion was similar to that in normal cortex [18]. That may be the reason that some cases had an indeterminate result using the perfusion imaging modalities, and a false-positive result using PET with FDG or radiolabeled amino acids. ^{13}N - NH_3 PET may solve such problem because the uptake of ^{13}N - NH_3 in brain tumors is governed by the capillary blood flow and metabolic properties of the tumor, and the perfusion and GS activity in the recurrent tumor are higher than in the

radiation injury. In this study, $^{13}\text{N-NH}_3$ PET was discordant with FDG PET in two contrast-enhanced lesions. The lesion with reactive gliosis and radiation necrosis showed less $^{13}\text{N-NH}_3$ uptake, however, slightly increased $^{18}\text{F-FDG}$ uptake in one contrast-enhanced lesion. One lesion with the recurrent anaplastic astrocytoma showed moderately increased $^{13}\text{N-NH}_3$ uptake, but less FDG uptake.

Conclusions

The recurrent astrocytomas showed increased $^{13}\text{N-NH}_3$ uptake, and the radiation necrosis showed absent or less $^{13}\text{N-NH}_3$ uptake, and $^{13}\text{N-NH}_3$ seem superior to $^{18}\text{F-FDG}$ for this purpose, suggesting that $^{13}\text{N-NH}_3$ is a promising tracer for separating radiation necrosis from astrocytoma recurrence. However, this is a pilot study with the selected patients, and the patient population was small. Thus, the further studies are needed to settle this issue.

Acknowledgment This work was partially supported by grant 031652 from the Nature Sciences Foundation of Guangdong Province, China.

References

1. Langlebe DD, Segall GM (2000) PET in differentiation of recurrent brain tumor from radiation injury. *J Nucl Med* 41:1861–1867
2. Janus TJ, Kim EE, Tilbury R et al (1993) Use of [^{18}F]fluorodeoxyglucose positron emission tomography in patients with primary malignant brain tumors. *Ann Neurol* 33:540–527
3. Ricci PE, Karis JP, Heiserman JE et al (1998) Differentiating recurrent tumor from radiation necrosis: time for re-evaluation of positron emission tomography? *Am J Neuroradiol* 9:407–413
4. Zhang X, Liang C, Chen W et al (2006) PET imaging of cerebral astrocytoma with ^{13}N -ammonia. *J Neurooncol* 78:145–151
5. Zhang X, Chen W, Zhou D (2005) ^{13}N -ammonia positron emission tomography in the diagnosis of astrocytomas: preliminary result. *J Nucl Med* 46(S):429
6. Kim CK, Alavi JB, Alavi A et al (1991) New grading system of cerebral gliomas using position emission tomography with F-18 fluorodeoxyglucose. *J Neurooncol* 10:85–91
7. Phelps ME, Huang SC, Hoffman EJ et al (1981) Cerebral extraction of N-13 ammonia: its dependence on cerebral blood flow and capillary permeability-surface area product. *Stroke* 12:607–619
8. Cooper AJL, McDonald JM, Gelbard AS et al (1979) The metabolic fate of ^{13}N -labeled ammonia in rat brain. *J Biol Chem* 254:4982–4992
9. Schelstraete K, Simons M, Deman J et al (1982) Uptake of ^{13}N -ammonia by human tumours as studied by positron emission tomography. *Br J Radiol* 55:797–804
10. Sugahara T, Korogi Y, Tomiguchi S et al (2000) Posttherapeutic intraaxial brain tumor: the value of perfusion-sensitive contrast-enhanced MR imaging for differentiating tumor recurrence from nonneoplastic contrast-enhancing tissue. *Am J Neuroradiol* 21:901–909
11. Tsui EY, Chan JH, Leung TW et al (2000) Radionecrosis of the temporal lobe: dynamic susceptibility contrast MRI. *Neuroradiology* 42:149–152
12. Schwartz RB, Carvalho PA, Alexander E et al (1991) Radiation necrosis vs high-grade recurrent glioma: differentiation by using dual-isotope SPECT with ^{201}Tl and $^{99\text{mTc}}$ -HMPAO. *Am J Neuroradiol* 12:1187–1192
13. Carvalho PA, Schwartz RB, Alexander E et al (1992) Detection of recurrent gliomas with quantitative thallium-201/technetium-99m HMPAO single-photon emission computerized tomography. *J Neurosurg* 77:565–570
14. Fucci L, Oliver CN, Coon MF et al (1983) Inactivation of key metabolic enzymes by mixed-function oxidation reactions: possible implication in protein turnover and ageing. *Pro Natl Acad Sci* 80:1521–1525
15. Pilkington GJ, Lantos PL (1982) The role of glutamine synthetase in the diagnosis of cerebral tumours. *Neuropathol Appl Neurobiol* 8:227–236
16. Akimoto J (1993) Immunohistochemical study of glutamine synthetase expression in normal human brain and intracranial tumors. *No To Shinkei* 45:362–368
17. McCormick D, McQuaid S, McCusker et al (1990) A study of glutamine synthetase in normal human brain and intracranial tumours. *Neuropathol Appl Neurobiol* 16:205–211
18. Spaeth N, Wyss MT, Weber B et al (2004) Uptake of ^{18}F -fluorocholine, ^{18}F -fluoroethyl-L-tyrosine, and ^{18}F -FDG in acute cerebral radiation injury in the rat: implications for separation of radiation necrosis from tumor recurrence. *J Nucl Med* 45:1931–1938